Meteoritics & Planetary Science 35, 1321-1331 (2000)

The South African polymict eucrite Macibini

P. C. BUCHANAN[1,2*], D. J. LINDSTROM[1], D. W. MITTLEFEHLDT[3], C. KOEBERL[4] AND W. U. REIMOLD[2]

[1]NASA Johnson Space Center, Mail Code SN2, Houston, Texas, USA 77058
[2]Department of Geology, University of the Witwatersrand, Private Bag 3, Wits 2050, Johannesburg, South Africa
[3]Mail Code C23, Lockheed Martin ESS, 2400 NASA Road 1, Houston, Texas, USA 77058
[4]Institute of Geochemistry, University of Vienna, Althanstrasse 14, A-1090 Vienna, Austria
*Correspondence author's e-mail address: 065pcb@cosmos.wits.ac.za

(Received 1999 December 7; accepted in revised form 2000 August 7)

Abstract–The polymict eucrite Macibini is a fragmental breccia, predominantly composed of eucritic materials with minor proportions (maximum 2 vol%) of diogenitic material. Hence, it is intermediate between the Yamato-74159-type polymict eucrites, which contain negligible amounts of magnesian orthopyroxene, and the howardites. The present study provides mineralogical and bulk compositional data for the meteorite breccia and for six clasts. These clasts include both volcanic and igneous rocks and a variety of impact-generated rocks. A broad range of degrees of postcrystallization metamorphism affected these materials before the final aggregation of the breccia.

Clast A is a fragment of unequilibrated eucrite with subophitic texture. The edges of the zoned pyroxenes in this clast are composed of a host of Fe-rich augite containing vermicules (blebs) and lamellae composed of a mixture of Fe-rich olivine and silica. Similar features occur as fragments in lunar breccias and are attributed by some workers to the breakdown of pyroxferroite, an Fe-rich pyroxenoid. However, textures and compositions of these augite-olivine-silica intergrowths in clast A suggest that, in this case, they are the result of decomposition in a series of steps of Fe-rich subcalcic augite.

Among the fragments of impact-generated material in Macibini is clast 2, an earlier-formed clastic breccia that was lithified before being broken apart and included in the meteorite breccia. Clast 3 is an impact-melt breccia that is composed of rock and mineral fragments in a devitrified groundmass. Clast C is also an impact-melt breccia that has a coarser-grained, hornfelsic groundmass that resulted from extensive metamorphism after formation.

INTRODUCTION

The meteorite Macibini fell on 1936 September 23, ~15 miles from Mtubatuba and 16 miles from Hlabisa near the present Hluhluwe/Umfolozi Game Reserve, Kwazulu Natal, Republic of South Africa (Haughton and Partridge, 1939). J. T. Barlow of Somkele observed the fall and details were reported in *The Natal Mercury*. Six fragments of the meteorite were found and weighed a total of ~2.0 kg. Haughton and Partridge (1939) gave the first scientific description, including mineralogical and some bulk compositional data. They classified Macibini as a eucrite and described it as a breccia containing rock fragments with ophitic textures. Jérome (1970) reported additional bulk compositional data and Reid (1974) noted that eucrite clasts within Macibini display a variety of textures and a range of compositions. The present study presents mineralogical and compositional data and some petrologic observations.

SAMPLING AND ANALYTICAL TECHNIQUES

Samples of the clasts and matrix of Macibini were extracted in the Meteorite Processing Facility at NASA Johnson Space Center (JSC) from a fragment of one of the stones that was provided by the Transvaal Museum, Pretoria, South Africa. Samples of five clasts were extracted from this fragment. The four matrix specimens were taken from different parts of the fragment and did not contain any obvious clasts. Subsamples of clasts and matrix were mounted as polished sections in the Thin Section Lab at JSC. Textures of matrix and clasts were documented by backscattered electron (BSE) images using a JEOL 6340 scanning electron microscope equipped for qualitative elemental analysis with an energy-dispersive system produced by IXRF Corp. and operated at 15 kV and a working distance of 14.9 mm. Mineral compositions were determined using the Cameca SX-100 electron microprobe at JSC. Approximate bulk compositions of fine-grained and glassy materials were determined using the microprobe with a beam rastered over an area of 50 × 50 μm. The microprobe was operated at a voltage of 15 kV and a sample current of 20 nA with counting times for individual elements ranging from 20–40 s. Natural and synthetic standards were used and corrections were made for absorption, fluorescence, and atomic number effects using Cameca on-line programs.

Bulk samples of several clasts and the matrix were analyzed by instrumental neutron activation analysis (INAA) at JSC using the procedures detailed in Mittlefehldt and Lindstrom (1991) and Mittlefehldt *et al.* (1992). These samples were irradiated for 12 h in the research reactor at the University of Missouri at a flux of ~5.5 × 10^{13} n/cm^2-s. Additional bulk samples of the matrix were analyzed by INAA at the Institute of Geochemistry, University of Vienna using the procedures described by Koeberl *et al.* (1987) and Koeberl (1993).

Disk-shaped samples of individual pyroxene and feldspar crystals were extracted from polished sections by a microcoring device. These sections were 100 μm thick and cores ranged from 0.43 to 0.50 mm in diameter for feldspars and 0.15 to 0.53 mm in diameter for pyroxenes. These samples were irradiated for 150 h in the flux trap of the research reactor at the University of Missouri at a flux of ~4 × 10^{14} n/cm^2-s and were analyzed for some major and trace elements in the Radiation Counting Laboratory at JSC using high-sensitivity, large intrinsic Ge detectors (55–59% efficiency). Typical count rates for plagioclase samples during these analyses were 100–2500 counts/s. Procedures and accuracies are discussed in Lindstrom *et al.* (1994).

DESCRIPTIONS

General Description

Macibini is composed of a fine-grained gray, brecciated matrix with a few lithic clasts of crystalline material. A black, glassy fusion crust covers the surface of the meteorite and is pitted and irregular. There is very little evidence of terrestrial alteration in the interior of the meteorite, except for minor amounts of iron oxide staining around metal grains. The following description of the matrix of the meteorite is based on examination of hand specimens and six thin sections with a combined area of ~6 cm^2. The matrix (Fig. 1) is predominantly composed of angular fragments of gray pyroxene and white plagioclase with minor amounts of silica, olivine, and opaque minerals. These opaque minerals include troilite and ilmenite with minor chromite and Fe-Ni metal. We did not find any individual fragments of phosphate minerals. Grain size of mineral fragments in these samples ranges from 1.5 mm to submicroscopic.

Matrix pyroxenes display a wide range of compositions (Fig. 2). Most of these mineral fragments apparently are derived from eucritic materials and are composed of a host of low-Ca pyroxene with one or more sets of augite exsolution lamellae. Some of these pyroxenes have undulatory extinction and exsolution lamellae that are deformed or displaced along intracrystalline fractures. In some cases, abundant, very small (<<1 μm) inclusions are oriented along host–lamellae boundaries. Similar inclusions were described and discussed by Harlow and Klimentidis (1980). The breccia also contains rare fragments of diogenitic orthopyroxene, which are, in some cases, relatively large (up to 0.8 mm in size) and are distinguished by moderate relief and low-order interference colors. These diogenitic fragments are unzoned and have no observable exsolution lamellae. Matrix feldspars are twinned and range in composition from Ab_5An_{95} to $Ab_{21}An_{77}$. Some of these feldspars contain small (<<1 μm) inclusions and display undulating extinction, deformation, and numerous fractures that displace twin boundaries.

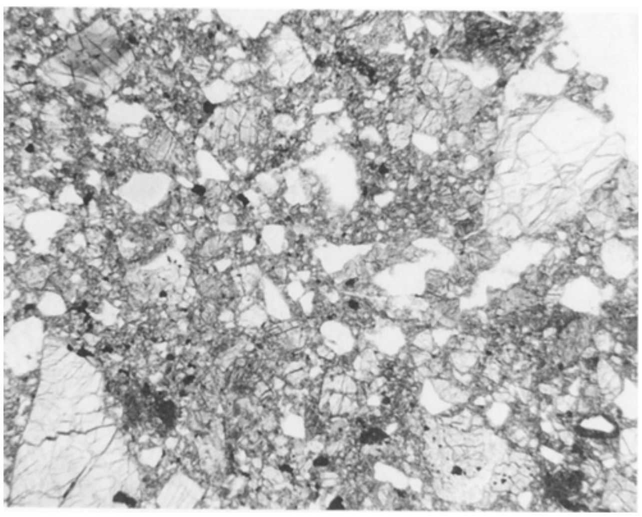

FIG. 1. Photomicrograph with transmitted light of the matrix breccia of Macibini. Long axis of the photo is 4 mm.

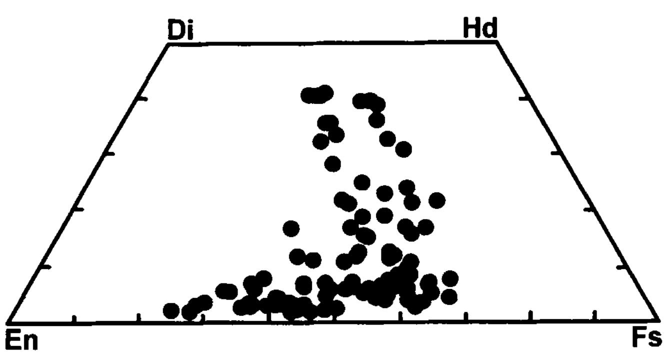

FIG. 2. Compositions of pyroxenes in the matrix of Macibini. These data represent electron microprobe analyses of the interiors of ~100 individual pyroxene fragments randomly chosen from the matrix of the meteorite.

The matrix of Macibini also contains small fragments of partially devitrified brown glass (maximum size 0.5 mm); representative compositions are listed in Table 1. These glass fragments are distinctive because they have higher abundances of K_2O than most eucrites (*e.g.*, Juvinas, 0.04 wt%; Kitts and Lodders, 1998). Abundances of K_2O are also greater than those of the matrix samples of Macibini (average 0.041 wt%; Table 2) and those of the fusion crust of the meteorite determined by electron microprobe (~0.04 wt%). These fragments are also enriched in K_2O relative to glass veins in Piplia Kalan (0.05 wt% K_2O; Buchanan *et al.*, 2000), glass fragments in Elephant Moriane (EET) 87509 (0.01–0.03 wt% K_2O; Buchanan, 1995), and glass veins in the eucrite Cachari (0.04–0.13 wt% K_2O; Bogard *et al.*, 1985). Glass fragments and spherules in the howardite Bununu also have lower abundances of K_2O (average 0.04 wt%; Noonan, 1974). In contrast, the glass and melt rocks in the howardite Malvern have similar K_2O abundances of 0.34–0.35 wt% (Noonan, 1974; Desnoyers and Jérome, 1977; Hewins and Klein, 1978).

Bulk compositions of all analyzed matrix samples of Macibini (Table 2) are similar in abundances of most major and trace elements. A weighted average of the compositions of the four samples analyzed for this study is similar to a more limited compositional data set for a bulk sample of Macibini reported by Jérome (1970). This average composition is slightly light rare earth element (LREE)-enriched with CI-normalized abundances of 13.6 for La and 11.9 for Lu (Fig. 3). There is a slight negative Eu anomaly with CI-normalized Eu/Sm of 0.92.

Clasts

Clast A–Clast A is >1 cm in diameter and is a fine- to medium-grained eucrite with subophitic texture composed of blocky to lath-shaped feldspars (up to 1.5 mm in size) and anhedral pyroxenes (up

TABLE 1. Representative compositions (wt%) of fragments of brown glass in the matrix of Macibini and of the devitrified matrix of clast 3.*

	Fragment 1	Fragment 2	Fragment 3	Clast 3 matrix
No. analyses	5	5	5	11
SiO_2	48.0	47.2	48.0	48.5
TiO_2	0.72	0.91	0.87	0.59
Al_2O_3	12.0	10.9	12.1	14.6
Cr_2O_3	0.41	0.41	0.36	0.17
FeO	18.2	20.3	18.1	17.9
MnO	0.59	0.61	0.59	0.55
MgO	8.38	7.88	7.47	5.50
CaO	10.2	10.2	11.3	10.7
Na_2O	0.19	0.10	0.24	1.24
K_2O	0.66	0.86	0.42	0.15
Total	99.3	99.4	99.4	99.9

*Compositions are averages of several individual electron microprobe analyses.

TABLE 2. Bulk compositions acquired by INAA of samples of the matrix of Macibini and of BHVO-1.

Lab	Sample 1a JSC	Sample 1b UV	Sample 2 UV	Sample 3 UV	Weighted average	BHVO-1 JSC
Weight (mg)	141.2	154.3	153.7	140.4	–	32.16
(wt%)						
Cr_2O_3	0.42	0.39	0.37	0.37	0.39	0.042
FeO	18.3	18.5	18.5	18.3	18.4	10.9
CaO	9.7	n.d.	n.d.	n.d.	–	11.0
Na_2O	0.46	0.48	0.46	0.43	0.46	2.31
K_2O	0.05	0.043	0.037	0.035	0.041	0.50
(ppm)						
Sc	29.3	31.1	29.4	29.2	29.8	31.4
Co	9.72	6.88	10.5	8.52	8.89	44.9
Ni	44	37	53	43	44	124
Zn	n.d.	3.2	2.6	2.4	2.7	n.d.
As	<0.20	0.5	0.2	0.6	0.4	0.5
Se	0.73	0.79	0.83	0.62	0.75	<0.6
Br	<0.31	0.17	0.33	0.25	0.25	<0.9
Rb	n.d.	0.66	<2	2	–	10
Sr	85	75	53	60	68	420
Zr	45	49	38	54	46	170
Sb	<0.047	0.025	0.039	0.018	0.028	0.15
Ba	30	45	33	32	35	140
La	3.00	3.57	3.26	3.11	3.24	15.3
Ce	8.68	9.68	8.93	8.21	8.89	38.0
Nd	6.3	6.31	6.05	5.58	6.07	24
Sm	1.897	2.17	1.92	1.86	1.97	6.15
Eu	0.618	0.74	0.72	0.66	0.69	2.06
Gd	n.d.	2.72	2.42	2.3	2.49	n.d.
Tb	0.465	0.512	0.433	0.414	0.457	0.93
Tm	n.d.	0.29	0.28	0.28	0.28	n.d.
Yb	1.85	1.99	1.94	1.84	1.91	2.00
Lu	0.274	0.315	0.31	0.29	0.298	0.273
Hf	1.38	2.04	1.39	1.44	1.57	4.65
Ta	0.172	0.23	0.17	0.18	0.19	1.15
Th	0.41	0.41	0.34	0.32	0.37	1.12
U	<0.18	0.11	0.1	0.07	0.09	0.41
(ppb)						
Ir	<4.4	0.6	0.8	0.7	0.7	<2.3
Au	<1.9	0.8	1.1	0.7	0.9	2.3

n.d. = not determined.
Abbreviations: JSC = Johnson Space Center, UV = University of Vienna.

to 1.2 mm in size) with minor ilmenite and olivine (Fig. 4). Pyroxenes in clast A are extensively zoned (Fig. 5) from clear magnesian cores (Wo_6En_{63}, Mg# 67) to dark brown, Ca- and Fe-rich edges ($Wo_{22}En_{21}$, Mg# 27) (Table 3). A very fine-grained (grain size down to 1 μm) mesostasis is composed of anhedral silica and ilmenite with minor feldspar and olivine. Lath-shaped crystals of a silica mineral also are present and are up to 1 mm in length and 0.2 mm in width (Fig. 6a). These crystals are composed of stacked sequences of thin plates giving them a comb-like shape in cross-section. Edges of these silica grains extend into surrounding feldspars and pyroxenes indicating that they began to crystallize before the mesostasis.

Takeda and Graham (1991) named the type of zoning of the pyroxenes in clast A the "Mg-Fe trend" and pointed out that this pattern commonly displays a "step" or moderate increase in Ca content on a compositional traverse from core to rim (Fig. 5) (see also Takeda *et al.*, 1983). The clast is a type 1 or 2 in degree of equilibration as defined by Takeda and Graham (1991). Fine, regularly spaced exsolution lamellae (<1 μm in width) are visible throughout the pyroxenes in clast A; pyroxene edges contain moderate numbers of inclusions. Feldspars are twinned, vary from clear to inclusion-rich, and range in composition from $Ab_{11}An_{89}$ to $Ab_{17}An_{81}$ (Table 3).

Two types of Fe-rich olivine occur in clast A in different textural associations. The first type of olivine has composition ~Fa_{80} (Table 4) and occurs in networks of irregular veinlets that are up to 20 μm in width and transect many of the zoned pyroxenes (Fig. 6b). Pyroxene in narrow zones (generally 5–10 μm wide)

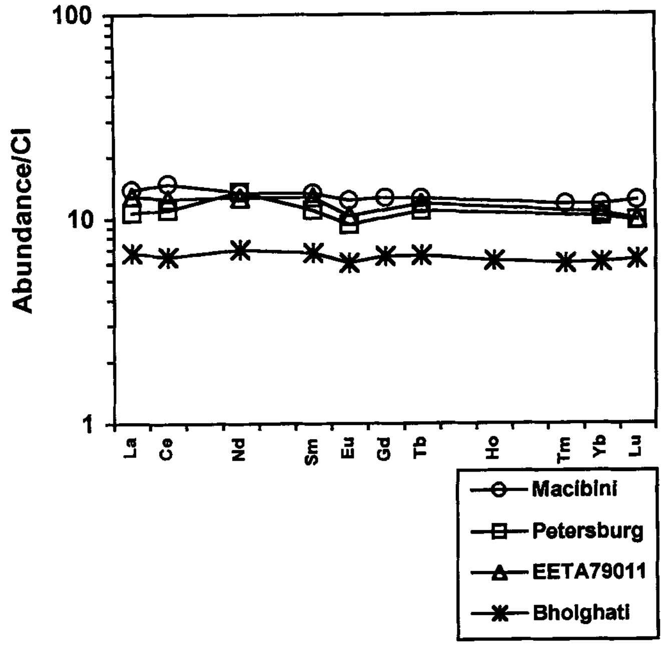

FIG. 3. The CI-normalized REE abundances in matrix samples of Macibini compared to other howardites and polymict eucrites. Data for Petersburg from Buchanan and Reid (1996), data for EETA79011 from Palme *et al.* (1983), data for Bholghati from Laul and Gosselin (1990). Abundances are normalized to mean CI composition (Anders and Grevesse, 1989).

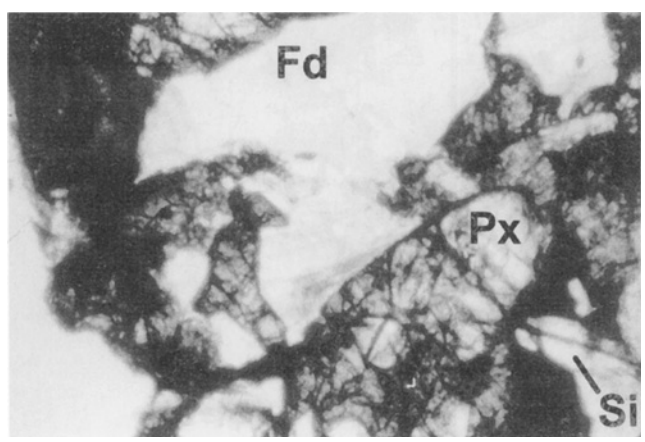

FIG. 4. Photomicrograph with transmitted light of a portion of clast A with feldspar (Fd), pyroxene (Px), and a silica mineral (Si). Long axis of the photo is 2.5 mm.

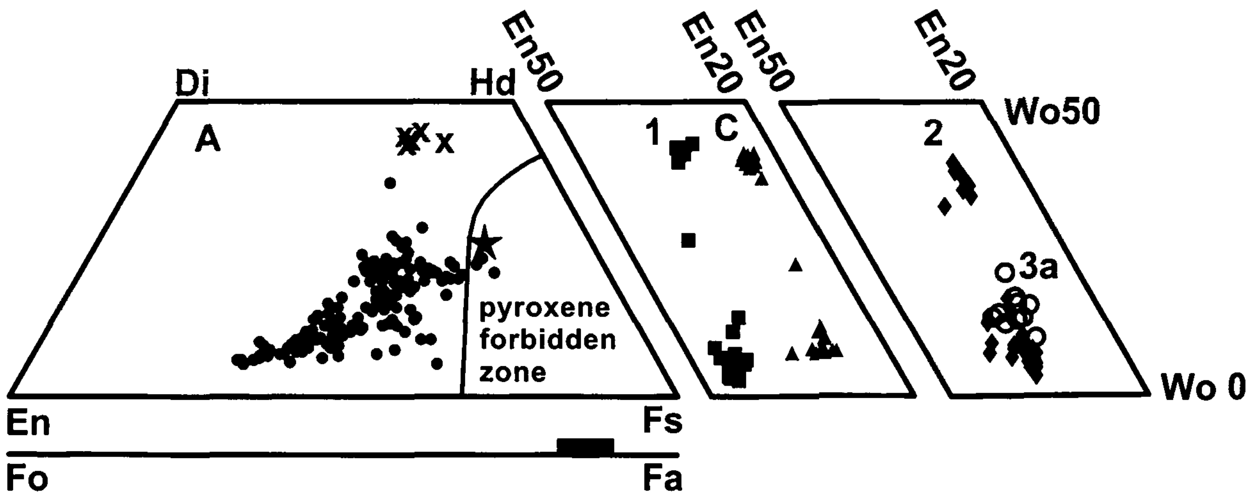

FIG. 5. Compositions of pyroxenes in Macibini clasts A, C, 1, 2, and 3a. For clast A, analyses (filled circles) were determined on traverses from centers to edges of zoned pyroxenes. The star represents the average of five rastered beam electron microprobe analyses of the augite-olivine-silica intergrowths at the edges of zoned pyroxenes; "x" represents the composition of the augite host. Compositional range of olivine in these intergrowths is plotted below the pyroxene quadrilateral. The approximate pyroxene forbidden zone (curved line in the lower right of the quadrilateral) is for 925 °C and one atmosphere pressure (Smith, 1972). Squares represent analyses of pyroxenes in clast 1, triangles are pyroxenes in clast C, diamonds are pyroxenes in clast 2, and open circles are pyroxenes in clast 3a.

TABLE 3. Representative pyroxene and plagioclase compositions (wt%) from clasts A, C, 1, and 3a from Macibini.

	Clast A			Clast C			Clast 1			Clast 3a		
	PX-1	PX-2	PL-1	PX-1	PX-2	PL-1	PX-1	PX-2	PL-1	PX-1	PX-2	PL-1
SiO_2	51.7	49.3	46.8	49.8	49.3	47.5	51.7	51.1	44.8	48.7	48.4	49.9
TiO_2	0.19	0.41	0.02	0.34	0.19	0.05	0.33	0.24	0.01	0.74	0.92	0.08
Al_2O_3	1.61	0.58	34.5	0.57	0.29	34.0	0.54	0.37	36.2	1.26	1.50	32.5
Cr_2O_3	0.81	0.19	n.d.	0.26	0.12	n.d.	0.23	0.21	n.d.	0.40	0.38	n.d.
FeO	20.3	21.9	0.48	20.9	36.8	0.88	15.1	30.4	0.72	30.1	26.9	0.77
MnO	0.71	0.57	n.d.	0.55	1.13	n.d.	0.57	0.88	n.d.	0.91	0.81	n.d.
MgO	20.7	6.52	0.14	8.24	9.33	n.d.	11.8	15.2	0.02	11.0	10.1	0.03
CaO	3.67	20.5	17.9	18.7	3.36	16.8	19.9	1.45	19.1	6.75	9.61	16.5
Na_2O	n.d.	n.d.	1.27	n.d.	n.d.	1.73	n.d.	n.d.	0.76	n.d.	n.d.	1.33
K_2O	n.d.	n.d.	0.09	n.d.	n.d.	0.20	n.d.	n.d.	0.02	n.d.	n.d.	0.10
Total	99.7	100.0	101.2	99.4	100.5	101.2	100.2	99.8	101.6	99.9	98.6	101.2
Mg#	64.5	34.6	–	41.3	31.1	–	58.4	47.2	–	39.5	40.1	–
Wo	7.6	44.0	–	40.2	7.46	–	41.4	3.1	–	14.8	21.5	–
En	59.6	19.4	–	24.7	28.8	–	34.2	45.7	–	33.7	31.5	–
Fs	32.8	36.6	–	35.1	63.7	–	24.4	51.2	–	51.5	47.0	–
An	–	–	88.1	–	–	83.3	–	–	93.2	–	–	86.8
Ab	–	–	11.3	–	–	15.5	–	–	6.7	–	–	12.6
Or	–	–	0.6	–	–	1.2	–	–	0.1	–	–	0.6

n.d. = not determined.

adjacent to these veinlets is altered to more Fe-rich compositions. The second type of Fe-rich olivine (Fig. 6c) occurs in the Ca- and Fe-rich edges of the zoned pyroxenes. These edges are composed of a host of Fe-rich augite ($Wo_{44}En_{18}$, Mg# 32) with vermicules (blebs) and lamellae that are up to 20 μm wide and are composed of a silica mineral intergrown with olivine of composition Fa_{82-90} (Table 4). Individual mineral grains within these blebs and lamellae are generally <5 μm in smallest dimension. Compositions of minerals in these augite-olivine-silica intergrowths are diagramed in Fig. 5. The approximate average composition of the augite-olivine-silica intergrowths was determined by rastered beam electron microprobe analysis and is similar to that of pyroxene of composition $Wo_{26}En_{16}$ (Mg# 22). This composition is on the same trend as the pyroxene zoning pattern but is within the approximate "forbidden zone" for pyroxenes at 925 °C and one atmosphere pressure (Smith, 1972).

The CI-normalized abundances of REE in clast A (Table 5) are slightly LREE-enriched (Fig. 7a) and are similar to those of Nuevo Laredo (Kitts and Lodders, 1998). There is a negative Eu anomaly with CI-normalized Eu/Sm of 0.76. In contrast, the abundance of Sc is similar to those of Juvinas and Stannern (Kitts and Lodders, 1998). On a plot of La *vs.* Sc (Fig. 8), bulk composition of clast A plots between main group eucrites and Stannern. Hence, the composition of the clast suggests that it may represent a proportion of partial melting intermediate between the main group eucrites and Stannern (Stolper, 1977).

TABLE 4. Representative compositions (wt%) of olivine in veins and augite-olivine-silica intergrowths from Macibini clast A.

	Vein olivine			Olivine from augite-olivine-silica intergrowths		
	OL-1	OL-2	OL-3	OL-4	OL-5	OL-6
SiO_2	31.0	30.9	30.8	30.6	30.5	30.7
TiO_2	0.02	0.02	0.02	0.06	0.07	0.03
Al_2O_3	0.03	0.01	n.d.	0.03	0.02	0.01
Cr_2O_3	0.05	0.09	0.01	n.d.	n.d.	0.01
FeO	59.5	58.9	59.7	63.1	62.1	60.4
MnO	1.37	1.36	1.31	1.42	1.45	1.32
MgO	7.72	7.70	7.99	4.38	5.41	7.26
CaO	0.09	0.11	0.03	0.22	0.22	0.27
Total	99.8	99.1	99.9	99.8	99.8	100.0
Fo	18.8	18.9	19.3	11.0	13.4	17.7
Fa	81.2	81.1	80.7	89.0	86.6	82.3

n.d. = not determined or below detection limits.

The centers of three feldspars, two pyroxenes, and an augite-olivine-silica intergrowth from a pyroxene edge were analyzed by micro-INAA (Table 6, Fig. 9a). Compositions of the plagioclase samples are LREE-enriched with CI-normalized abundances of 1 for La compared to 0.15 for Lu, and a CI-normalized Eu/Sm of 16. Compositions of the centers of pyroxenes are similar to those in other unequilibrated eucrites (*e.g.*, Pasamonte; Pun and Papike, 1996) and are only slightly less magnesian than orthopyroxenes in diogenites. These pyroxene centers are LREE-depleted with CI-normalized abundances of 0.1 for La and 0.6 for Lu. Abundances of Eu are below detection limits. Composition of the augite-olivine-silica intergrowth is extremely ferroan and is greatly enriched in REE compared to the centers of pyroxenes. This intergrowth is slightly LREE enriched with CI-normalized abundances for La of 9 and for Lu of 8. A slight negative Eu anomaly is present with CI-normalized Eu/Sm of 0.8. These data are consistent with progressive crystallization of a eucritic melt.

Clast A is a fragment of volcanic rock that has undergone little postcrystallization metamorphism and is probably most similar to the unmetamorphosed Antarctic clast Yamato (Y)-75011,84 (*e.g.*, Takeda *et al.*, 1994). Yamato-75011,84 is a fragment of mesostasis-rich, subophitic basalt with extensive zoning of pyroxene from magnesian pigeonite cores to subcalcic ferroaugite rims (Takeda *et al.*, 1983, 1994). Silica laths occur in the mesostasis of this clast (Arai *et al.*, 1998a) and veinlets containing Fe-rich olivine transect pyroxenes and are similar in texture to those in clast A (Takeda *et al.*, 1994). However, augite-olivine-silica intergrowths have not been reported in Y-75011,84.

Fragments of Fe-rich augite with blebs and lamellae of olivine and silica are relatively common in lunar rocks (*e.g.*, Snyder *et al.*, 1999) and are similar in texture and mineral compositions to the augite-olivine-silica intergrowths of clast A. These lunar fragments have been interpreted as the result of the decomposition of pyroxferroite, a yellow Fe-rich pyroxenoid found in lunar rocks (*e.g.*, Lindsley *et al.*, 1972). Chao *et al.* (1970) report a composition of $(Fe_{0.84}Ca_{0.13}Mg_{0.02}Mn_{0.02})(Si_{0.99}Al_{0.01})O_3$ for this pyroxenoid. Lindsley and Burnham (1970) produced synthetic pyroxferroite of a similar composition $(Ca_{0.15}Fe_{0.85}SiO_3)$. In contrast, the average composition of the augite-olivine-silica intergrowths in clast A is significantly richer in Ca ($\sim Wo_{26}En_{16}$). Although rastered beam electron microprobe analysis is not an ideal analytical technique, the

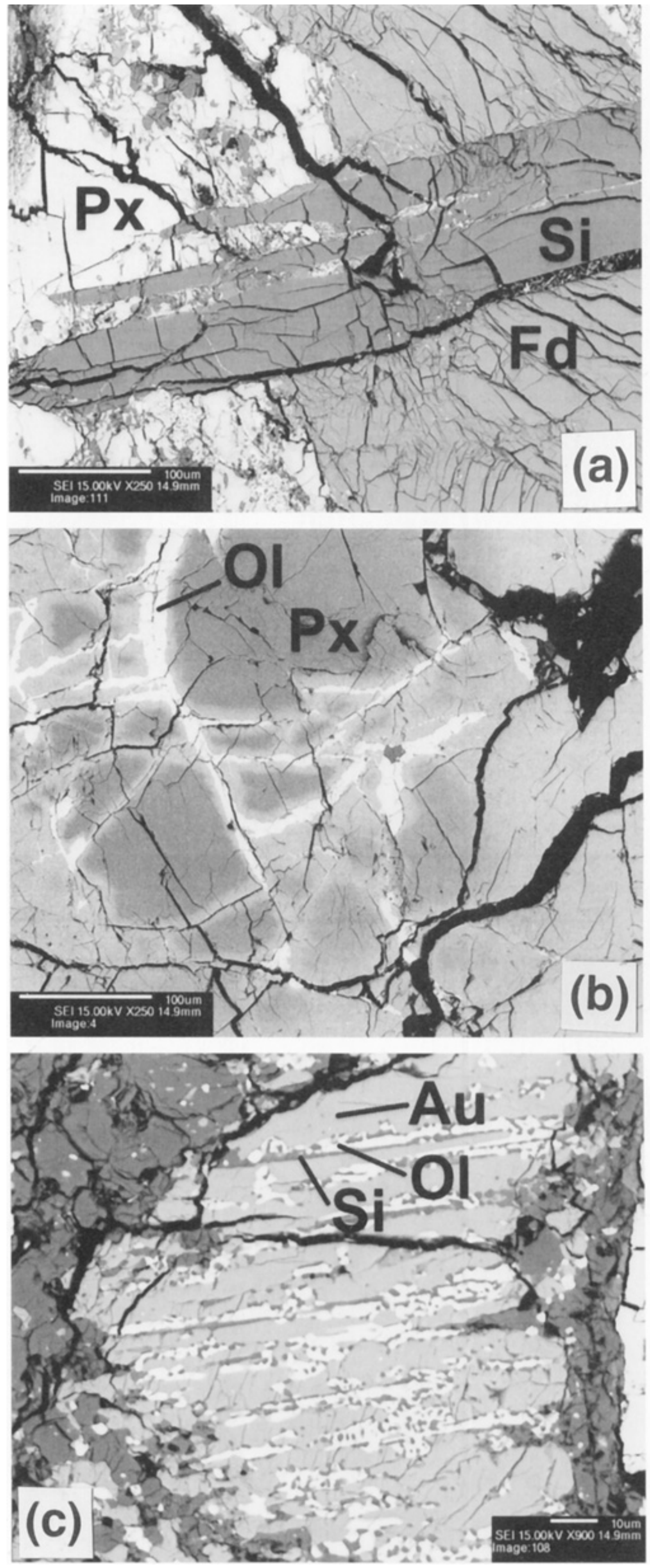

FIG. 6. (a) Backscattered electron image of a grain of a silica mineral (Si), in contact with pyroxene (Px) and feldspar (Fd) grains. Scale bar is 100 μm. (b) Backscattered electron image of Fe-rich olivine (Ol) in veinlets transecting zoned pyroxene crystals (Px). Scale bar is 100 μm. (c) Backscattered electron image of the edge of a zoned pyroxene with a host of augite (Au) and lamellae composed of a mixture of Fe-rich olivine (Ol) and a silica mineral (Si). Scale bar is 10 μm.

TABLE 5. Bulk compositions acquired by INAA of samples of clasts from Macibini.

	Clast A	Clast C	Clast 1	Clast 2	Clast 3
Weight (mg)	68.8	62.1	84.3	113.6	154.8
(wt%)					
Cr_2O_3	0.326 ± 0.004	0.251 ± 0.003	0.169 ± 0.002	0.354 ± 0.004	0.344 ± 0.004
FeO	18.8 ± 0.2	18.8 ± 0.2	6.71 ± 0.07	17.4 ± 0.2	18.4 ± 0.2
CaO	10.2 ± 0.5	10.0 ± 0.5	15.2 ± 0.4	10.1 ± 0.4	10.0 ± 0.5
Na_2O	0.603 ± 0.008	0.588 ± 0.007	0.682 ± 0.008	0.434 ± 0.005	0.658 ± 0.008
K_2O	0.08 ± 0.03	0.10 ± 0.02	<0.09	<0.06	0.09 ± 0.04
(ppm)					
Sc	30.4 ± 0.3	35.1 ± 0.4	10.8 ± 0.1	27.8 ± 0.3	31.0 ± 0.3
Co	5.35 ± 0.06	5.91 ± 0.07	1.99 ± 0.02	5.73 ± 0.07	5.65 ± 0.07
Ni	n.d.	n.d.	<10	n.d.	n.d.
As	<1.7	<0.23	<0.29	<0.25	0.52 ± 0.13
Se	<0.4	0.84 ± 0.26	<0.15	n.d.	0.63 ± 0.20
Br	<0.25	n.d.	0.19 ± 0.07	<0.30	0.29 ± 0.07
Sr	94 ± 14	110 ± 17	122 ± 6	59 ± 17	85 ± 13
Zr	55 ± 17	97 ± 20	<31	49 ± 16	50 ± 19
Sb	<0.48	<0.05	0.029 ± 0.007	<0.032	<0.044
Cs	n.d.	n.d.	<0.015	n.d.	n.d.
Ba	49 ± 7	66 ± 8	20 ± 3	29 ± 5	31 ± 6
La	3.94 ± 0.05	6.11 ± 0.08	0.846 ± 0.015	2.79 ± 0.04	3.36 ± 0.04
Ce	10.8 ± 0.2	15.8 ± 0.4	2.06 ± 0.07	8.53 ± 0.22	9.5 ± 0.5
Nd	6.4 ± 2.4	11.4 ± 2.5	<3.1	4.3 ± 1.9	6.9 ± 1.6
Sm	2.46 ± 0.03	3.75 ± 0.05	0.287 ± 0.005	1.76 ± 0.02	2.08 ± 0.03
Eu	0.714 ± 0.013	0.905 ± 0.018	0.747 ± 0.010	0.612 ± 0.012	0.588 ± 0.012
Tb	0.590 ± 0.019	0.857 ± 0.026	0.063 ± 0.004	0.420 ± 0.018	0.493 ± 0.018
Yb	2.26 ± 0.04	3.44 ± 0.06	0.272 ± 0.012	1.78 ± 0.03	1.88 ± 0.04
Lu	0.330 ± 0.010	0.494 ± 0.013	0.041 ± 0.002	0.258 ± 0.007	0.280 ± 0.008
Hf	1.91 ± 0.05	3.02 ± 0.08	0.189 ± 0.014	1.29 ± 0.04	1.65 ± 0.05
Ta	0.245 ± 0.012	0.398 ± 0.018	0.018 ± 0.003	0.162 ± 0.011	0.189 ± 0.012
Th	0.436 ± 0.023	0.68 ± 0.03	0.030 ± 0.010	0.32 ± 0.04	0.350 ± 0.021
U	0.11 ± 0.05	0.24 ± 0.05	<0.07	0.08 ± 0.04	<0.19
(ppb)					
Ir	n.d.	n.d.	<1.1	n.d.	n.d.
Au	<1.8	<2.1	2.4 ± 0.5	<1.6	<2.2

n.d. = not determined.

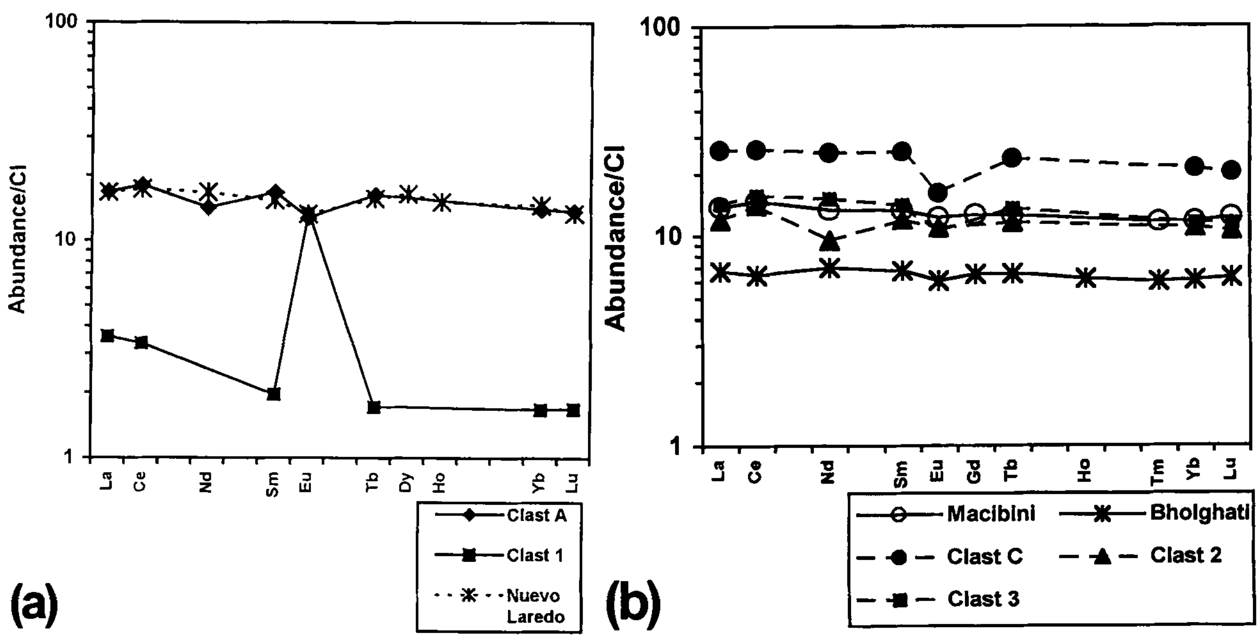

FIG. 7. Rare earth element diagrams for bulk compositions of clasts from Macibini. Abundances are normalized to mean CI composition (Anders and Grevesse, 1989). (a) Igneous-volcanic materials: clast A (filled diamonds) and clast 1 (filled squares). Also included are the chondrite-normalized element abundances of Nuevo Laredo (Kitts and Lodders, 1998). (b) Impact-related materials: clasts C, 2, and 3 compared with bulk compositions of Macibini and Bholghati (howardite). Data for Macibini from this study; data for Bholghati from Laul and Gosselin (1990).

striking difference in normative wollastonite content between this average composition and the composition of pyroxferroite suggests that the edges of the zoned pyroxenes in clast A were originally Fe-rich subcalcic augite and not pyroxferroite.

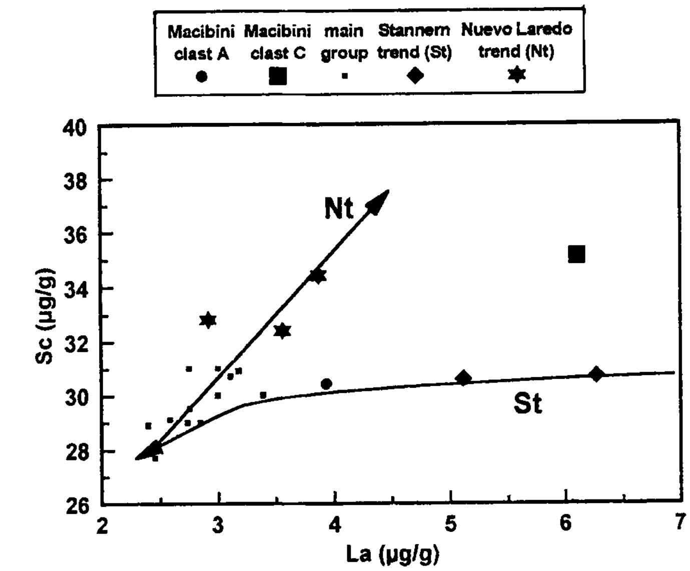

FIG. 8. Plot of Sc (ppm) *vs.* La (ppm) comparing Macibini clasts with "main group" (small filled squares), Stannern trend (filled diamonds), and Nuevo Laredo trend (stars) eucrites. Clast A is represented by a filled circle and clast C is represented by a large filled square. Data are from this study and Mittlefehldt (pers. comm.).

Textures and mineral compositions suggest that with further cooling after crystallization, this Fe-rich subcalcic augite exsolved into a host of augite containing vermicules and lamellae of low-Ca pyroxene. These vermicules and lamellae decomposed at lower temperatures to a mixture of Fe-rich olivine and silica. The significant proportions of CaO in this olivine suggest that the low-Ca pyroxene originally contained in these lamellae may have been pigeonite (as also suggested by H. Takeda, pers. comm., 1998), rather than orthopyroxene. However, these olivines are very fine-grained and the elevated proportions of CaO may be the result of beam overlap into the surrounding augite host.

Clast C–Clast C (>5.5 mm in diameter) is composed of irregular xenoliths and xenocrysts in a fine-grained groundmass with an average grain size of <30 μm (Fig. 10a). The groundmass has an equigranular texture and consists of pyroxene, feldspar, silica, and abundant grains of opaque minerals, including ilmenite. In some cases, equant pyroxenes and feldspars in this groundmass are arranged in chains of grains that apparently are the result of recrystallization of lath-shaped crystals. Xenoliths and xenocrysts are up to 1 mm in size and are composed of pyroxenes and feldspars that are coarser-grained than those in the groundmass. All of the pyroxenes in the clast are equilibrated and are composed of varying proportions of augite exsolution lamellae ($Wo_{40}En_{25}$) in a low-Ca pyroxene host (Wo_7En_{29}) (Table 3, Fig. 5). Feldspars in the clast have a compositional variation of $Ab_{12-22}An_{77-86}$ (Table 3). Clast C is rich in incompatible trace elements (Table 5) with abundances of REE that are somewhat greater than those of Stannern (Kitts and Lodders, 1998). The clast is LREE-enriched with CI-normalized

TABLE 6. Bulk compositions determined by microanalytical INAA of the centers of pyroxenes (PX) and feldspars (PL) from clasts A and 1 and of an augite-olivine-silica intergrowth (AOS) from clast A.

	Clast 1			Clast A					
	PL1	PL2	PX1	PL1	PL2	PL3	PX1	PX2	AOS
(wt%)									
FeO	0.075	0.16	27.1	0.52	0.56	0.60	3.53	4.65	14.8
CaO	12.5	17.9	3.31	17.5	15.7	17.6	0.68	0.72	6.6
Na_2O	0.54	0.90	0.068	1.22	1.33	1.35	0.005	0.007	0.27
K_2O	0.027	0.037	0.006	0.07	0.12	0.09	n.d.	n.d.	0.013
(ppm)									
Sc	0.100	0.281	37.6	0.223	0.206	0.246	5.89	7.92	23.3
Cr	7.48	7.76	2219	17.4	15.2	19.3	807	1106	1300
Co	0.292	0.060	5.63	4.84	2.32	2.95	1.38	1.92	4.36
Ni	n.d.	n.d.	n.d.	n.d.	n.d.	n.d.	n.d.	n.d.	24
Zn	0.87	0.00	74	1.60	n.d.	1.62	2.1	4.9	35.5
Rb	0.17	n.d.	n.d.	0.48	n.d.	0.29	n.d.	n.d.	n.d.
Sr	107	156	n.d.	153	155	148	n.d.	n.d.	56
Sb	0.011	0.013	n.d.	0.021	n.d.	0.030	n.d.	n.d.	n.d.
Ba	19.2	29.7	n.d.	11.4	26.7	16.8	n.d.	n.d.	17
La	0.646	0.664	0.204	0.197	0.172	0.296	0.022	0.035	2.18
Ce	1.41	1.61	1.06	0.40	0.45	0.57	0.20	0.27	7.18
Sm	0.157	0.203	0.291	0.142	0.140	0.143	0.034	0.044	1.41
Eu	0.657	0.940	0.090	0.832	0.950	0.867	n.d.	n.d.	0.45
Tb	0.008	0.007	0.104	0.010	0.007	0.008	0.015	n.d.	0.323
Yb	0.014	0.019	0.681	0.025	n.d.	0.026	0.094	0.122	1.32
Lu	n.d.	n.d.	0.109	0.0041	n.d.	0.0032	0.0131	0.0164	0.194
Hf	n.d.	n.d.	0.39	n.d.	n.d.	n.d.	n.d.	n.d.	0.86
Ta	n.d.	n.d.	n.d.	n.d.	n.d.	n.d.	n.d.	n.d.	0.15
Th	n.d.	n.d.	0.077	n.d.	n.d.	n.d.	n.d.	n.d.	0.20
(ppb)									
Au	n.d.	n.d.	n.d.	0.0025	n.d.	n.d.	n.d.	n.d.	0.0032

n.d. = not determined.

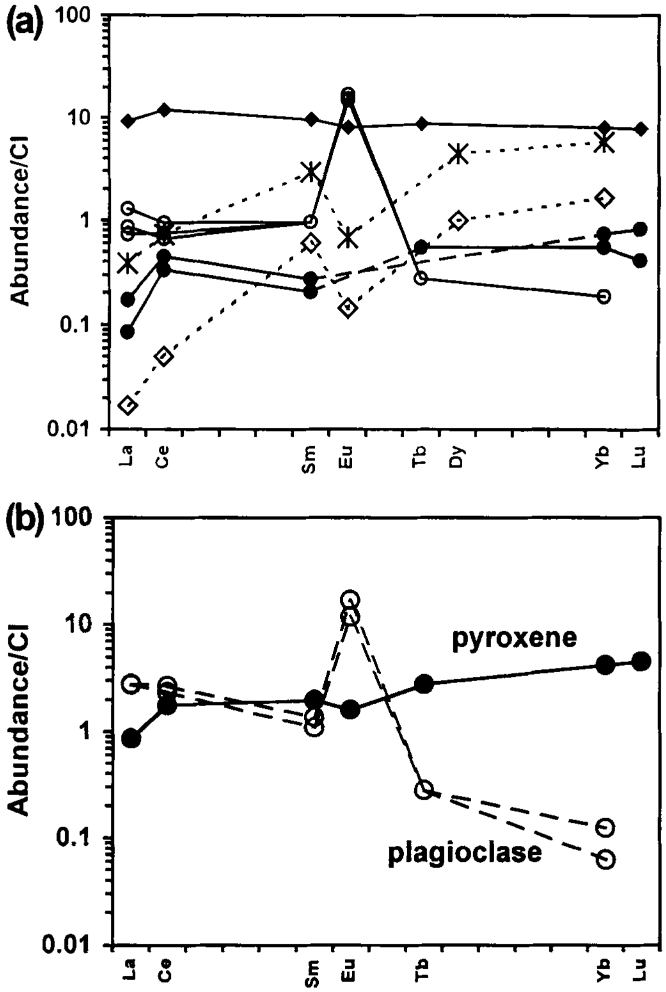

FIG. 9. (a) Rare earth element diagram for the compositions of minerals from clast A. Included are the centers of feldspars (open circles, solid lines) and pyroxenes (filled circles, solid lines) and the edge of a pyroxene grain with augite-olivine-silica intergrowth (filled diamonds, solid lines). Abundances of Eu are below detection limits for the centers of pyroxene grains. Also included are chondrite-normalized element abundances of the center (open diamonds, dashed lines) and edge (stars, dashed lines) of a pyroxene from the unequilibrated eucrite Pasamonte (Pun and Papike, 1996). Eu abundance of the center is a maximum. (b) Rare earth element diagram for the centers of feldspars (open circles) and pyroxenes (filled circles) from clast 1. Data for both diagrams are normalized to mean CI composition (Anders and Grevesse, 1989).

abundances of La at 26 and of Lu at 20 (Fig. 7b). The clast has a negative Eu anomaly with CI-normalized Eu/Sm of 0.63.

Clast C is a metamorphosed impact-melt breccia with irregular rock and mineral fragments in a groundmass that originally was glassy or fine-grained. Metamorphism apparently recrystallized this groundmass to equant mineral grains. Similar textures are seen in lithology C of the Indian eucrite Piplia Kalan (Buchanan *et al.*, 2000). The texture of the groundmass of clast C is also similar, in some respects, to that of the unbrecciated eucrite Ibitira, which originally had a variolitic texture and was subsequently recrystallized (Steele and Smith, 1976). However, it must be noted that the grain size of Ibitira is much greater than that of the groundmass of clast C. The composition of clast C does not plot on the Nuevo Laredo trend or the Stannern trend on a plot of La *vs.* Sc (Fig. 8) and is consistent with an impact-generated mixture of a variety of eucritic materials from both trends.

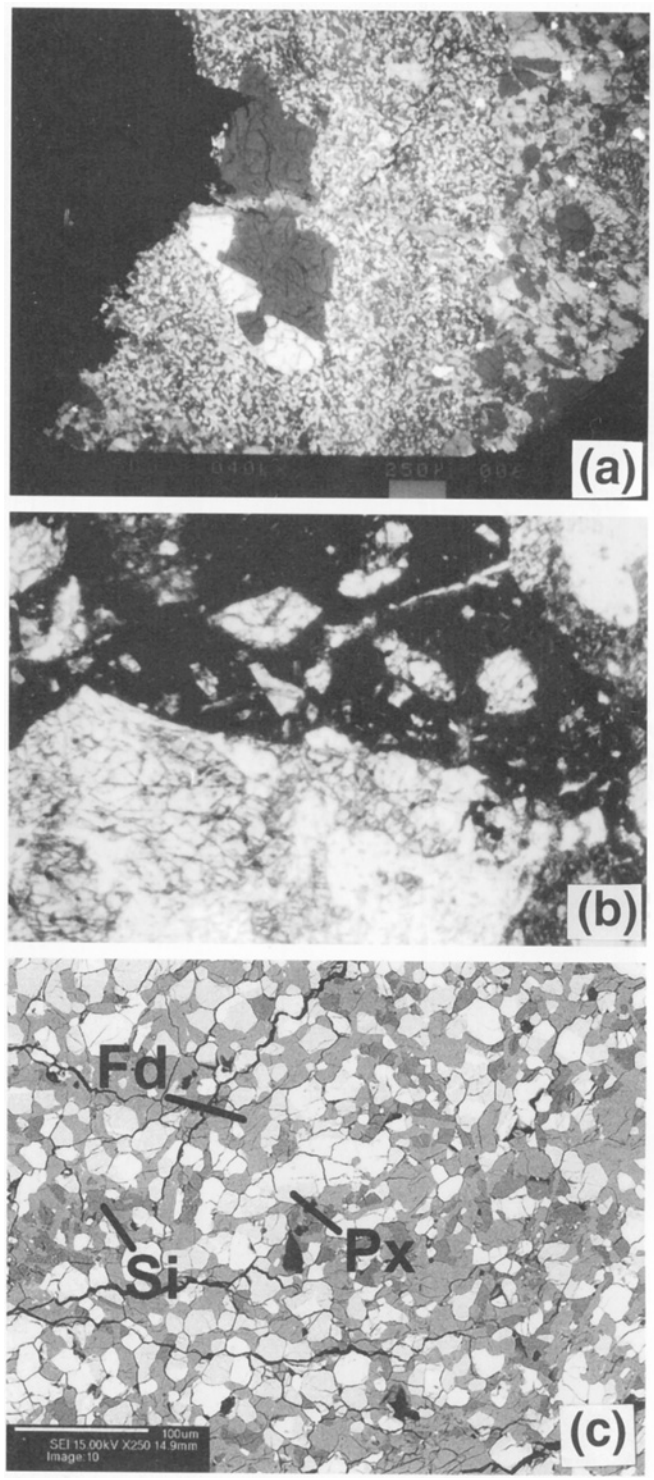

FIG. 10. (a) Backscattered electron image of Macibini clast C. Pyroxene is light gray; feldspar is dark gray. Note xenolith composed of coarser-grained pyroxene and plagioclase in a finer-grained groundmass. Scale bar is 250 μm. (b) Photomicrograph with transmitted light of a portion of clast 3, including mineral and rock fragments in a dark, devitrified groundmass. Long axis of the photo is 2.5 mm. (c) Backscattered electron image of Macibini clast 3a. Scale bar is 100 μm.

Clast 1–Clast 1 is composed of pyroxene and plagioclase with grain size >2 mm. Textural information is limited because fragments of the clast in thin section are relatively small compared to the grain size. Feldspars have mosaic textures and compositions that are relatively uniform, varying from Ab_6An_{94} to Ab_9An_{91} (Table 3). Pyroxenes are inclusion-rich and are partially recrystallized to fine-grained, equigranular textures. These pyroxenes are composed of relatively fine augite exsolution lamellae in a low-Ca pyroxene host. Microprobe analyses range from Wo_3En_{46} to $Wo_{43}En_{32}$ (Table 3; Fig. 5) and represent mixtures of varying proportions of low-Ca and high-Ca phases.

The clast is slightly LREE-enriched with CI-normalized abundances of La at 3.60 and of Lu at 1.65 (Fig. 7a); it has a large positive Eu anomaly with CI-normalized Eu/Sm of 6.84. Compositions of the cores of plagioclase grains (Table 6; Fig. 9b) are more LREE-enriched than plagioclase in clast A with CI-normalized abundances of La at 2.8 and of Yb at 0.1. The CI-normalized Eu/Sm of 11.6 indicates a large positive Eu anomaly. The composition of the core of a pyroxene is richer in REE than those of the cores of pyroxenes from clast A and has a pattern that is LREE-depleted with CI-normalized abundances of La at 0.9 and of Lu at 4.5 (Fig. 9b). A small negative Eu anomaly is present with CI-normalized Eu/Sm of 0.8.

The medium to coarse-grain size of clast 1 and its mineral compositions, which include anorthite-rich plagioclase and pyroxene more magnesian than that of Juvinas (BVSP, 1981), suggest that this clast may be a fragment of a cumulate eucrite. Trace element abundances of the minerals in this clast also are similar to those of cumulate eucrites. Composition of the pyroxene that was analyzed by micro-INAA is more similar to those in Moama than to those in Juvinas or in unequilibrated eucrites, including Pasamonte and Y-75011,84 (Hamet *et al.*, 1978; Pun and Papike, 1996; Arai *et al.*, 1998b). Compositions of the feldspar grains are intermediate in REE abundances between those in Moama and Serra de Magé and those in Moore County (Hamet *et al.*, 1978; Ma and Schmitt, 1979; Pun *et al.*, 1997). However, several pieces of evidence do not support classification of clast 1 as a fragment of cumulate eucrite. The fineness of the augite exsolution lamellae in the pyroxenes of this clast and the inclusions that they contain are not typical of cumulate eucrites (*e.g.*, Lovering, 1975). Hence, it is also possible that this clast is a fragment of a noncumulate eucrite that is more magnesian than main group eucrites.

Several points about the bulk composition of clast 1 are noteworthy. Abundances of FeO and of incompatible trace elements are low (Table 5). Scandium content is much lower than those of noncumulate eucrites (*e.g.*, Juvinas, Stannern, and Nuevo Laredo) or cumulate eucrites (*e.g.*, Moore County) (Kitts and Lodders, 1998). However, the very high abundance of CaO (15.2 wt%) compared to those of noncumulate eucrites (*e.g.*, Juvinas, 10.7 wt%; Kitts and Lodders, 1998) and cumulate eucrites, including Serra de Magé, Moore County, and Moama (11.1, 10.3, and 9.47 wt%, respectively; Kitts and Lodders, 1998; Lovering, 1975), suggest that this sample was unrepresentative and contained larger proportions of plagioclase than the original rock. This is a reasonable interpretation considering the small sample size and the coarse-grained character of the clast. In comparison, multiple analyses of "whole rock" samples of relatively coarse-grained eucrites have previously displayed considerable variations. For example, the reported Al_2O_3 contents of Serra de Magé range from 12.7 to 20.9 wt% (Jarosewich, 1990; McCarthy *et al.*, 1973) reflecting variations in plagioclase/pyroxene in the sampled material.

Clast 2–Clast 2 is >4.5 mm in diameter and represents a fragment of a clastic breccia predominantly composed of mineral fragments of pyroxene and feldspar with minor olivine, silica, and opaque minerals, including ilmenite. The breccia is fine-grained (grain size up to 0.75 mm) and mineral fragments commonly have equant shapes. The clast has very little porosity and apparently was lithified with recrystallization of very fine-grained mineral fragments. Pyroxenes range in composition from Wo_8En_{56} to $Wo_{13}En_{34}$. Most of these pyroxenes are equilibrated with fine exsolution lamellae in a low-Ca pyroxene host. Feldspar fragments are twinned and range in composition from Ab_7An_{93} to $Ab_{20}An_{79}$. The CI-normalized REE abundances of a bulk sample of the clast (Table 5; Fig. 7b) are almost flat with La at 11.9 and Lu at 10.6. The CI-normalized Eu/Sm of 0.91 indicates a slight negative Eu anomaly.

Clast 2 represents a preexisting breccia that was lithified and later broken apart with fragments included in the final meteorite breccia. Composition of the clast is similar to that of the matrix of the meteorite (Table 2). Abundances of REE are similar to those of polymict eucrites and more REE-rich than howardites (Fig. 7b). Abundances of other trace elements are also similar to those of polymict eucrites (*e.g.*, Petersburg; Buchanan and Reid, 1996).

Clast 3–Clast 3 is ~2 cm in diameter and is composed of irregular rock and mineral fragments (50 vol%) in a groundmass composed of devitrified brown glass (50 vol%) (Fig. 10b). Mineral fragments include both pyroxenes and feldspars, many of which display evidence of deformation, including undulating extinction. Among the rock fragments contained in the clast are several large eucrite fragments that are composed of blocky feldspar and anhedral pyroxene with ophitic–subophitic texture and average grain size of <1 mm. The largest of these fragments is 9 × 6 mm in size. Compositions of pyroxenes in rock and mineral fragments range from Wo_7En_{41} to $Wo_{36}En_{29}$. Compositions of feldspars range from Ab_6An_{93} to $Ab_{15}An_{84}$. The devitrified glass of the groundmass contains dendritic to equigranular crystals that are extremely fine-grained (down to $<<1\,\mu m$ in size) and include pyroxene and feldspar. Average composition of the groundmass (based on 11 rastered beam electron microprobe analyses) is listed in Table 1. Composition (Table 5) of a bulk sample of the clast without large rock and mineral fragments is slightly LREE-enriched with CI-normalized abundances of La at 14.3 and of Lu at 11.5 (Fig. 7b). The CI-normalized Eu/Sm of 0.74 indicates a small negative Eu anomaly.

Clast 3 is a fragment of impact-melt breccia that is composed of irregular rock and mineral fragments in a devitrified impact melt. Bulk composition of the clast is similar to those of many polymict eucrites (*e.g.*, EETA79011; Palme *et al.*, 1983). Most elemental abundances are similar to those of bulk Macibini (Jérome, 1970) or matrix samples of Macibini (Table 2). These data suggest that clast 3 resulted from impact melting of the same regolithic material represented in the matrix of the meteorite. Hewins and Klein (1978), Metzler and Stöffler (1995), and Pun *et al.* (1998) described similar impact-melt breccias in howardites and polymict eucrites. The devitrified texture of the groundmass of clast 3 indicates that this material has undergone some metamorphism.

Clast 3a–Two fragments of clast 3a were found in the same thin section as clast 3. Bulk samples were not available. The larger fragment is 6 × 2 mm in size, whereas the smaller fragment is 3 × 1.5 mm in size. The clast has a fine-grained texture (grain size $<100\,\mu m$) and is composed of pyroxene, feldspar, silica, and opaque minerals (Fig. 10c). Pyroxenes are equilibrated and are composed of fine augite exsolution lamellae (<1 μm) in a low-Ca host; exsolution lamellae are so fine compared to the excitation volume of the electron microprobe beam that analyses display a very limited range in composition from $Wo_{13}En_{36}$ to $Wo_{22}En_{31}$ (Table 3; Fig. 5). These pyroxenes are commonly equant in shape. Feldspars are also equant and have a limited compositional range of $Ab_{12-14}An_{84-87}$ (Table 3).

The fine-grained, equigranular texture of clast 3a is similar to the metamorphosed groundmass of clast C (this study) and to the metavolcanic lithology C in the eucrite Piplia Kalan (Buchanan *et al.*, 2000). This texture is also similar to terrestrial volcanic rocks that were metamorphosed (Buchanan *et al.*, 2000). Eucrite clasts with granoblastic textures were described in the howardite Kapoeta by Pun *et al.* (1998). Clast 3a apparently represents a fragment of fine-grained or glassy eucritic material that has been recrystallized.

DISCUSSION

The variety of compositions of mineral fragments and clasts in Macibini confirm the suggestion by Reid (1974) that the meteorite is a polymict breccia. Petrographic analysis and the compositions of matrix pyroxenes (Fig. 2) indicate that it contains a maximum of 2 vol% diogenitic material and, hence, is a polymict eucrite (Delaney *et al.*, 1983a). The bulk composition of Macibini confirms this classification. Abundance of CaO is similar to those of most polymict eucrites (*e.g.*, Petersburg; Buchanan and Reid, 1996) and is greater than those of most howardites (*e.g.*, Frankfort; Jérome, 1970). The howardites, which contain larger proportions of diogenitic orthopyroxene than the polymict eucrites, have smaller proportions of Ca-rich feldspar and augite and, hence, lower CaO content. Abundances of REE in Macibini also are similar to those of polymict eucrites and greater than those of howardites (Fig. 3). Larger proportions of diogenitic materials, which are relatively depleted in REE compared to eucrites, result in lower abundances of these elements in the howardites compared to the polymict eucrites. Macibini is intermediate between the Y-74159-type polymict eucrites (*e.g.*, Y-75011), which contain negligible proportions of diogenitic material (*e.g.*, Takeda *et al.*, 1983), and the howardites.

Despite the fact that individual clasts in Macibini vary in bulk composition and texture, the matrix samples analyzed in this study and the bulk meteorite sample analyzed by Jérome (1970) are similar in composition. This similarity suggests that these data accurately represent the bulk composition of the meteorite and are not affected by unrepresentative sampling of some components (*e.g.*, phosphates). Because these matrix and bulk samples were taken from different parts of the meteorite, impact processes apparently mixed the regolith well.

Two of the clasts considered in this study are materials that are most easily attributed to volcanic–igneous processes. Clast A is an unequilibrated eucrite and clast 1 is a eucrite that is more magnesian than main group eucrites. In contrast, several clasts from this meteorite have features that are most easily attributed to impact. Clast C and clast 3 are impact-melt breccias. Clast 2 is a lithified clastic breccia. Fragments of pyroxene and feldspar in the matrix of Macibini are derived from a variety of materials that are represented, at least in part, by the lithic clasts analyzed in this study. Although most of these mineral fragments are probably derived from igneous–volcanic materials, the rock clasts found in this meteorite suggest that some of these mineral and glass fragments are derived from materials that were formed or modified by impact.

Materials contained within Macibini also display a wide spectrum of degrees of postcrystallization metamorphism. Clasts range from unmetamorphosed to extensively recrystallized. Clast A is unequilibrated and is probably similar in texture, chemical composition, and mineral chemistry to the original volcanic rock from which it was derived. Clast 3 is an impact-melt breccia that has been mildly metamorphosed with devitrification of glass. In contrast, Clast C is an impact-melt breccia that has been extensively recrystallized to a hornfelsic texture. Clast 3a has a similar texture to other metavolcanic eucritic materials. The variation in the degree of equilibration of these materials indicates that metamorphism occurred in large part before the final aggregation of the meteorite. A schematic petrogenetic history of the materials contained within Macibini is presented in Table 7.

Macibini is similar, in many respects, to the meteorite Kapoeta, which also contains fragments of a variety of impact-related materials, including earlier-formed clastic breccias and impact-melt breccias (Pun *et al.*, 1998). Pun (1992) described an unmetamorphosed eucrite fragment (clast E) in the howardite Kapoeta that is similar to clast A of Macibini. However, in contrast to Macibini, which is a polymict eucrite, Kapoeta is a howardite with significant proportions of diogenitic orthopyroxene in the brecciated matrix.

The high abundances of K_2O in the fragments of brown glass in the matrices of Macibini and Malvern are difficult to explain (see also Desnoyers and Jérome, 1977). These abundances (0.15–0.86 wt% K_2O) are greater than those of most eucrites or glasses found in other howardite, eucrite, and diogenite (HED) breccias. One possible explanation is that these glasses are impact melts that are composed of a mixture of eucritic material and an impactor. However, other types of meteorites that might have impacted the surface of the HED parent body do not generally have high abundances of K_2O. Another possible explanation is that these glasses are impact melts that contain a significant component of K_2O-rich eucritic mesostasis material.

CONCLUSIONS

(1) Macibini is a polymict eucrite that contains minor proportions of diogenitic orthopyroxene and is intermediate between the Y-74159-type polymict eucrites, which contain negligible proportions of diogenitic material, and the howardites, which contain >10% diogenitic material (Takeda *et al.*, 1983; Delaney *et al.*, 1983b).

(2) Based on the textures, mineral compositions, and bulk compositions of the clasts analyzed in this study, Macibini contains a variety of materials that were formed by both volcanic and impact processes. Some of these materials are relatively unmetamorphosed, whereas others have been extensively recrystallized. Hence, metamorphism occurred before final aggregation of the breccia.

(3) Clast A is a relatively unmetamorphosed eucrite and is similar to a clast of Y-75011,84 (*e.g.*, Takeda *et al.*, 1994). This clast is a member of the Stannern-trend with composition that is intermediate between those of the main group eucrites and Stannern. Relatively

TABLE 7. Schematic petrogenetic history of Macibini with petrographic evidence.

Crystallization	Ophitic/subophitic textures of clast A. Zoning of minerals in clast A. Crystallization of clast 1.
Brecciation	Formation of breccia (clast 2) and impact-melt breccia (clast 3). This event may have been associated with mild metamorphism that devitrified the glassy matrix of clast 3. The temporal relationship with the metamorphism that recrystallized clasts 2, 3a, and C is unclear.
Metamorphism	Equilibration of minerals. Recrystallization of material in clasts 2, 3a, and C.
Final brecciation	Final structure of the meteorite.

unmetamorphosed eucritic materials are not limited to Y-75011 and the Y-74159-type polymict eucrites but also occur in other HED polymict breccias (Delaney *et al.*, 1984).

(4) The presence of Fe-rich augite-olivine-silica intergrowths at the edges of zoned pyroxenes in clast A indicates that these features can form by closed-system crystallization of relatively mafic melts. These intergrowths apparently formed by the decomposition in a series of steps of Fe-rich subcalcic augite. Not all Fe-rich olivines in meteorites of the HED association are direct crystallization products from eucritic melts.

Acknowledgments-The Transvaal Museum, South Africa, kindly provided samples of Macibini with permission of the Chief Director of the Council for Geoscience (Dr. Frick) and with the support of Mr. Patrick Bender (Curator of Geology). Part of this work was supported by the Austrian FWF, project Y58-GEO, to C. K. Support was also provided by the Foundation for Research Development of the Republic of South Africa to W. U. R. This work was performed while P. C. B. held a National Research Council-JSC Research Associateship. Analytical support at JSC was provided under grant RTOP 344-31-10-17 to D. J. L. This is the University of the Witwatersrand Impact Cratering Research Group contribution number 17. The authors appreciate the insightful reviews provided by Aurora Pun and Akira Yamaguchi and the editorial assistance of Hiroko Nagahara.

Editorial handling: H. Nagahara

REFERENCES

ANDERS E. AND GREVESSE N. (1989) Abundances of the elements: Meteoritic and solar. *Geochim. Cosmochim. Acta* **53**, 197–214.

ARAI T., TAKEDA H., LOFGREN G. E. AND MIYAMOTO M. (1998a) Metamorphic transformations of opaque minerals in some eucrites. *Antarctic Meteorite Res.* **11**, 71–91.

ARAI T., TAKEDA H., PAPIKE J. J., SHEARER C. K. AND MIYAMOTO M. (1998b) Rare-earth-element abundance of pyroxene and plagioclase in a pristine eucritic basalt, Yamato 75011,84 (abstract). *Meteorit. Planet. Sci.* **33 (Suppl.)**, A10.

BOGARD D. D., TAYLOR G. J., KEIL K., SMITH M. R. AND SCHMITT R. A. (1985) Impact melting of the Cachari eucrite 3.0 Gy ago. *Geochim. Cosmochim. Acta* **49**, 941–946.

BUCHANAN P. C. (1995) Petrology of five howardites and polymict eucrites: Bholghati, Petersburg, EET 87509, EET 87513, EET 87531. Ph. D. thesis, Univ. Houston, Houston, Texas, USA. 313 pp.

BUCHANAN P. C. AND REID A. M. (1996) Petrology of the polymict eucrite Petersburg. *Geochim. Cosmochim. Acta* **60**, 135–146.

BUCHANAN P. C., MITTLEFEHLDT D. W., HUTCHISON R., KOEBERL C., LINDSTROM D. J. AND PANDIT M. K. (2000) Petrology of the Indian eucrite Piplia Kalan. *Meteorit. Planet. Sci.* **35**, 609–615.

BVSP (BASALTIC VOLCANISM STUDY PROJECT) (1981) *Basaltic Volcanism on the Terrestrial Planets*. Pergamon, New York, New York, USA. 1286 pp.

CHAO E. C. T. *ET AL.* (1970) Pyroxferroite, a new calcium-bearing iron silicate from Tranquillity Base. *Proc. Apollo 11 Lunar Sci. Conf.* 65–79.

DELANEY J. S., PRINZ M., NEHRU C. E. AND HARLOW G. E. (1983a) The nomenclature of the polymict basaltic achondrites. *Meteoritics* **18**, 103–111.

DELANEY J. S., TAKEDA H. AND PRINZ M. (1983b) Modal comparison of Yamato and Allan Hills polymict eucrites. *Mem. Natl. Inst. Polar Res., Spec.Issue* **30**, 206–223.

DELANEY J. S., PRINZ M. AND TAKEDA H. (1984) The polymict eucrites. *Proc. Lunar Planet. Sci. Conf. 15th, J. Geophys. Res.* **89 (Suppl.)**, C251–C288.

DESNOYERS C. AND JÉROME D. Y. (1977) The Malvern howardite: A petrological and chemical discussion. *Geochim. Cosmochim. Acta* **41**, 81–86.

HAMET J., NAKAMURA N., UNRUH D. M. AND TATSUMOTO M. (1978) Origin and history of the adcumulate eucrite, Moama as inferred from REE abundances, Sm-Nd and U-Pb systematics. *Proc. Lunar Planet. Sci. Conf.* **9th**, 1115–1136.

HARLOW G. E. AND KLIMENTIDIS R. (1980) Clouding of pyroxene and plagioclase in eucrites: Implications for post-crystallization processing. *Proc. Lunar Planet. Sci. Conf.* **11th**, 1131–1148.

HAUGHTON S. H. AND PARTRIDGE F. C. (1939) The meteorite fall of Macibini, Zululand. *Trans. Geol. Soc. South Africa* **41**, 205–210.

HEWINS R. H. AND KLEIN L. C. (1978) Provenance of metal and melt rock textures in the Malvern howardite. *Proc. Lunar Planet. Sci. Conf.* **9th**, 1137–1156.

JAROSEWICH E. (1990) Chemical analyses of meteorites: A compilation of stony and iron meteorite analyses. *Meteoritics* **25**, 323–337.

JÉROME D. Y. (1970) Composition and origin of some achondritic meteorites. Ph.D. thesis, Univ. Oregon, Eugene, Oregon, USA. 167 pp.

KITTS K. AND LODDERS K. (1998) Survey and evaluation of eucrite bulk compositions. *Meteorit. Planet. Sci.* **33 (Suppl.)**, A197–A213.

KOEBERL C. (1993) Instrumental neutron activation analysis of geochemical and cosmochemical samples: A fast and proven method for small sample analysis. *J. Radioanal. Nucl. Chem.* **168**, 47–60

KOEBERL C., KLUGER F. AND KIESL W. (1987) Rare earth element determinations at ultratrace abundance levels in geologic materials. *J. Radioanal. Nucl. Chem.* **112**, 481–487

LAUL J-C. AND GOSSELIN D. C. (1990) The Bholghati howardite: Chemical study. *Geochim. Cosmochim. Acta* **54**, 2167–2175.

LINDSLEY D. H. AND BURNHAM C. W. (1970) Pyroxferroite: Stability and x-ray crystallography of synthetic $Ca_{0.15}Fe_{0.85}SiO_3$ pyroxenoid. *Science* **168**, 364–367.

LINDSLEY D. H., PAPIKE J. J. AND BENCE A. E. (1972) Pyroxferroite: Breakdown at low pressure and high temperature (abstract). *Lunar Sci.* **3**, 483–485.

LINDSTROM D. J., WENTWORTH S. J., MARTINEZ R. R. AND MCKAY D. S. (1994) Trace element identification of three chemically distinct very low titanium (VLT) basalt glasses from Apollo 17. *Geochim. Cosmochim. Acta* **58**, 1367–1375.

LOVERING J. F. (1975) The Moama eucrite—A pyroxene-plagioclase adcumulate. *Meteoritics* **10**, 101–114.

MA M-S. AND SCHMITT R. A. (1979) Genesis of the cumulate eucrites Serra de Magé and Moore County: A geochemical study. *Meteoritics* **14**, 81–89.

MCCARTHY T. S., ERLANK A. J. AND WILLIS J. P. (1973) On the origin of eucrites and diogenites. *Earth Planet. Sci. Lett.* **18**, 433–442.

METZLER K. AND STÖFFLER D. (1995) Impact melt rocks and granulites from the HED asteroid (abstract). *Meteoritics* **30**, 547.

MITTLEFEHLDT D. W. AND LINDSTROM M. M. (1991) Generation of abnormal trace element abundances in Antarctic eucrites by weathering processes. *Geochim Cosmochim. Acta* **55**, 77–87.

MITTLEFEHLDT D. W., SEE T. H. AND HÖRZ F. (1992) Dissemination and fractionation of projectile materials in the impact melts from Wabar Crater, Saudi Arabia. *Meteoritics* **27**, 361–370.

NOONAN A. F. (1974) Glass particles and shock features in the Bununu howardite. *Meteoritics* **9**, 233–242.

PALME H., SPETTEL B., BURGHELE A., WECKWERTH G., WÄNKE H., DELANEY J. S. AND PRINZ M. (1983) Elephant Moraine polymict eucrites; a eucrite-howardite compositional link (abstract). *Lunar Planet. Sci.* **14**, 590–591.

PUN A. (1992) Kapoeta: Implications for the igneous history and regolith evolution of the HED parent body. M. Sc. thesis, Univ. New Mexico, Albuquerque, New Mexico, USA. 171 pp.

PUN A. AND PAPIKE J. J. (1996) Unequilibrated eucrites and the equilibrated Juvinas eucrite: Pyroxene REE systematics and major, minor, and trace element zoning. *Am. Mineral.* **81**, 1438–1451.

PUN A., PAPIKE J. J. AND LAYNE G. D. (1997) Subsolidus REE partitioning between pyroxene and plagioclase in cumulate eucrites: An ion microprobe investigation. *Geochim. Cosmochim. Acta* **61**, 5089–5097.

PUN A., KEIL K., TAYLOR G. J. AND WEILER R. (1998) The Kapoeta howardite: Implications for the regolith evolution of the howardite-eucrite-diogenite parent body. *Meteorit. Planet. Sci.* **33**, 835–851.

REID A. M. (1974) The Macibini meteorite and some thoughts on the origin of basaltic achondrites. *Meteoritics* **9**, 398–399.

SMITH D. (1972) Stability of iron-rich pyroxene in the system $CaSiO_3$–$FeSiO_3$–$MgSiO_3$. *Am. Mineral.* **57**, 1413–1428.

SNYDER G. A., TAYLOR L. A. AND PATCHEN A. (1999) Lunar meteorite EET 96008, Part I. Petrology & mineral chemistry: Evidence of large-scale, late-stage fractionation (abstract). *Lunar Planet. Sci.* **30**, #1499, Lunar and Planetary Institute, Houston, Texas, USA (CD-ROM).

STEELE I. M. AND SMITH J. V. (1976) Mineralogy of the Ibitira eucrite and comparison with other eucrites and lunar samples. *Earth Planet. Sci. Lett.* **33**, 67–78.

STOLPER E. (1977) Experimental petrology of eucritic meteorites. *Geochim. Cosmochim. Acta* **41**, 587–611.

TAKEDA H. AND GRAHAM A. L. (1991) Degree of equilibration of eucritic pyroxenes and thermal metamorphism of the earliest planetary crust. *Meteoritics* **26**, 129–134.

TAKEDA H., WOODEN J. L., MORI H., DELANEY J. S., PRINZ M. AND NYQUIST L. E. (1983) Comparison of Yamato and Victoria Land polymict eucrites: A view from mineralogical and isotopic studies. *Proc. Lunar. Planet. Sci. Conf. 14th, J. Geophys. Res.* **88 (Suppl.)**, B245–B256.

TAKEDA H., MORI H. AND BOGARD D. D. (1994) Mineralogy and ^{39}Ar–^{40}Ar age of an old pristine basalt: Thermal history of the HED parent body. *Earth Planet. Sci. Lett.* **122**, 183–194.